

# In Situ Luminescence Probing of the Chemical and Structural Changes during Formation of Dip-Coated Lamellar Phase Sodium Dodecyl Sulfate Sol–Gel Thin Films

Michael H. Huang,<sup>†</sup> Bruce S. Dunn,<sup>\*,‡</sup> and Jeffrey I. Zink<sup>\*,†</sup>

Contribution from the Departments of Chemistry and Biochemistry and Materials Science and Engineering, University of California, Los Angeles, California 90095

Received November 1, 1999

**Abstract:** Sodium dodecyl sulfate (SDS)-templated sol–gel films formed by the rapid dip-coating method possess highly ordered lamellar phase structure. Thin film morphology allows both the chemistry and the dynamics of the assembly process to be traced in real time because the steps involved in the formation of the mesostructured material are separated both spatially and temporally. The dynamic processes that occur during film formation can be conveniently monitored by the combination of interferometry and luminescence spectroscopy of the incorporated molecular probes. The luminescence of the probe molecule is measured with a spatial resolution of 100  $\mu\text{m}$ . The selected probes respond to changes in the surrounding solvent composition and polarity, and report these changes by changes in their luminescence characteristics. In situ luminescence spectra taken at various stages during the film formation process monitor changes in the solvent composition, onset of micelle formation, and its transformation to the final mesophase structure. Local molecular motion in the dried films is also examined.

## Introduction

Recent developments in the preparation of surfactant-templated mesostructured sol–gel silica materials have extended the morphology from the originally discovered powders, with particle sizes on the order of microns,<sup>1</sup> to continuous thin films.<sup>2</sup> Mesostructured sol–gel thin films formed by the rapid dip-coating method have been made with hexagonal, lamellar, and cubic structures that possess a high degree of long-range order.

Thin-film morphology not only allows macroscopic materials to be fabricated, but also enables both the chemistry and the dynamics of the assembly process to be traced in real time because the steps involved in the formation of the mesostructured material are separated both spatially and temporally.<sup>3–5</sup> The starting point of the process is a solution containing all of

the components that assemble to form the final solid. All of the steps leading to the final material, including micelle formation and the hydrolysis and condensation reactions that form the silica, occur above the sol as the substrate is pulled from the liquid. As the substrate is withdrawn at a constant rate from the solution, the processes occur at different heights and times; the spatial separation enables the various stages of the process to be interrogated.

To monitor the changes in the solvent composition and the micelle and mesophase formation during the dip-coating process, luminescent probe molecules that can be incorporated in the material at all stages of the processing are used. The probe molecules are chosen to probe a particular aspect of the film-forming process. Luminescent molecules that respond to the changes in the solvent composition, for example, can interrogate the dynamic changes that occur in real time as the film is pulled. Other probe molecules are chosen to probe the polarity of the medium or its rigidity in their immediate environment, and thus interrogate the system in real time about the formation of micelles. The interrogation is nondestructive, and low concentrations of the probe molecules do not perturb the processing dynamics.

The film formation process starts with a solution of the silica precursor (a tetraalkoxysilane), solvent (water and alcohol), surfactant (in surfactant-templated films), and catalyst (HCl). In the dip-coating process, a substrate (silicon or silica) is slowly withdrawn from the sol reservoir. The moving substrate entrains the sol, forming an initially liquid film. The film thins by solvent evaporation and gravitational draining. When the upward moving flux is balanced by that of the evaporation, a steady film profile, 1 to 2 cm in height, is established. The film profile is wedge-shaped until it reaches a thickness beyond which it is essentially constant.<sup>6–8</sup> Concurrent with this process is the formation of both silica and micelles and their transformation

<sup>†</sup> Department of Chemistry and Biochemistry.

<sup>‡</sup> Department of Materials Science and Engineering.

(1) (a) Kresge, C. T.; Leonowicz, M. E.; Roth, W. J.; Vartuli, J. C.; Beck, J. S. *Nature* **1992**, 359, 710. (b) Beck, J. S.; Vartuli, J. C.; Roth, W. J.; Leonowicz, M. E.; Kresge, C. T.; Schumitt, K. D.; Chu, C. T.-W.; Olson, D. H.; Sheppard, E. W.; McCullen, S. B.; Higgins, J. B.; Schlenker, J. L. *J. Am. Chem. Soc.* **1992**, 114, 10834.

(2) (a) Ogawa, M. *J. Am. Chem. Soc.* **1994**, 116, 7941. (b) Yang, H.; Kuperman, A.; Coombs, N.; Maniche-Afara, S.; Ozin, G. A. *Nature* **1996**, 379, 703. (c) Yang, H.; Combs, N.; Sokolov, I.; Ozin, G. A. *Nature* **1996**, 381, 589. (d) Aksay, I. A.; Trau, M.; Manne, S.; Honma, I.; Yao, N.; Zhou, L.; Fenter, P.; Eisenberger, P. M.; Gruner, S. M. *Science* **1996**, 273, 892. (e) Tolbert, S. H.; Schäffer, T. E.; Feng, J.; Hansma, P. K.; Stucky, G. D. *Chem. Mater.* **1997**, 9, 1962. (f) Martin, J. E.; Anderson, M. T.; Odinek, J. G.; Newcomer, P. P. *Langmuir* **1997**, 13, 4133. (g) Ryoo, R.; Ko, C. H.; Cho, S. J.; Kim, J. M. *J. Phys. Chem B* **1997**, 101, 10610. (h) Martin, J. E.; Anderson, M. T.; Odinek, J.; Newcomer, P. *Langmuir* **1997**, 13, 4133. (i) Ogawa, M.; Kikuchi, T. *Adv. Mater.* **1998**, 10, 1077.

(3) Lu, Y.; Ganguli, R.; Drewien, C. A.; Anderson, M. T.; Brinker, C. J.; Gong, W.; Guo, Y.; Soye, H.; Dunn, B.; Huang, M. H.; Zink, J. I. *Nature* **1997**, 389, 364.

(4) Huang, M. H.; Dunn, B. S.; Soye, H.; Zink, J. I. *Langmuir* **1998**, 14, 7331.

(5) Sellinger, A.; Weiss, P. M.; Nguyen, A.; Lu, Y.; Assink, R. A.; Gong, W.; Brinker, C. J. *Nature* **1998**, 394, 256.

into the ordered mesostructure. The thickness of the film can be measured optically by using interferometry. By simultaneously combining spectroscopy of the luminescent molecular probes with interferometry, both the dynamic chemical and structural changes that occur during the dip-coating mesostructured film formation process can be followed.

The dynamic properties of particular importance in this study are the changes in film thickness, solvent composition, and micelle formation as a function of time. The thickness is monitored in all cases by interferometry. When the substrate is withdrawn from the solution at a constant rate, a steady state develops in a few seconds in which the film thickness at a given height above the solution remains constant even though the substrate is moving. The interference fringes remain constant in the dynamic system. The film thickness at a given height and thus at a given time in the formation process is measured. Simultaneously, the luminescence of the probe molecule is measured with a spatial resolution of 100  $\mu\text{m}$  (corresponding to a temporal resolution of about 0.1 s). The solvent composition is measured in two ways: the ratio of the intensities of two luminescence peaks is quantitatively related to the alcohol:water ratio, and the ratio of the intensities of two vibronic bands in the luminescence spectrum is quantitatively related to the solvent polarity. Solvent composition in a sol without addition of surfactant is measured as a control; the changes caused by the presence of the surfactant on the solvent composition can then be interpreted. The formation of micelles is measured by the ratio of the intensities of two vibronic bands in the luminescence spectrum when the probe molecule is incorporated in the hydrophobic part of the micelle.

In all cases, the interrogations are made on dynamically evolving systems in real time. The spatial resolution of the experiments is determined by the spot size of the laser probe beam (100  $\mu\text{m}$  or less) and the thickness of the film ranges from 1500 Å in final dried films to 30 000 Å near the solution reservoir. The properties of the final SDS sol–gel films are also reported. Molecular motion continues for several hours after the film has been pulled.

In this paper, we use these optical methods to examine the film formation process of dip-coated SDS-templated sol–gel film system. Silica films templated by SDS form highly ordered lamellar mesostructure. We report the synthesis, structural characterization, and dynamic processes of lamellar mesostructured films. We begin the discussion of the probe studies with a comparison of the evolution of solvent composition during the film formation process in the presence and absence of surfactant. A ternary composition diagram is given to show the changes in the depositing films that lead to the final silica films. Next, we discuss the lamellar mesostructured film formation process. Finally, we show that local molecular motion continues in the fresh dried film for several hours, although no measurable changes are observed in the X-ray diffraction pattern.

## Experimental Section

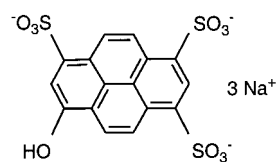
**Materials Preparation, and Film Characterization.** SDS-templated sol–gel silica films possess a highly ordered lamellar-phase structure. The development of solvent composition and the structural evolution of the mesostructured film formation were probed by pyranine and pyrene, respectively. The sol was prepared by refluxing TEOS (Aldrich),

ethanol, water, and HCl (mole ratio: 1:3.8:1:5  $\times 10^{-5}$ ) at 60 °C for 90 min. This forms the stock solution,<sup>9</sup> designed to minimize the siloxane condensation rate.<sup>10</sup> Typically 0.3 mL of deionized water and 0.9 mL of 0.07 N HCl were added to 7.5 mL of the stock solution to increase the concentration of HCl to 7.34 mM. The sol was stirred for 15 min and then aged for another 15 min at room temperature for both steps, followed by a dilution with 2 equiv of ethanol. To the sol was then added 0.5–2 wt % (0.014–0.057 M) SDS. The final molar proportions of the constituents were 1:22.3:5.1:0.004:0.023–0.092 TEOS/ethanol/H<sub>2</sub>O/HCl/SDS. A sol prepared the same way, but without the addition of SDS, was made to monitor the changes in the solvent composition during film formation. Pyranine (Sigma Chemical Co.) was then added to give a final concentration of  $1 \times 10^{-4}$  M, or pyrene (Eastman Kodak Co.) was added to give a final concentration of between  $1 \times 10^{-4}$  and  $2 \times 10^{-4}$  M. For the measurement of molecular motion in the fresh dried SDS sol–gel films  $2 \times 10^{-4}$  M BBAN, a phosphorescent probe (provided by Gerard Marriott), was added to the sol.

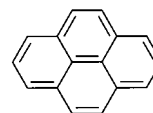
The films were drawn using the equipment described previously that uses hydraulic motion to produce a steady and vibration-free withdrawal of substrate from the sol.<sup>8</sup> Polished Si (100) substrates (9 cm  $\times$  1 cm  $\times$  1 mm) were cleaned with Nochromix (Godax Laboratories Inc.) and then rinsed with and stored in deionized water prior to use. These substrates were connected, through a ribbon, to a weighted float in a cylindrical water tank whose drainage was controlled by a flow valve. On top of the sol reservoir a transparent Pyrex cover was placed to reduce the air current and to slow the evaporation rate. Convection-free drying was critical to obtaining high optical quality films. A small opening on the Pyrex cover allows the passage for the excitation laser and collection of the probe emission. For all the probe studies, the films were withdrawn at a speed of 5 cm/min. A steady fringe pattern was established within 15 s after the start of the experiment and persisted until the bottom of the substrate was pulled from the sol ( $\sim 2$  min). After film deposition, thicknesses of some dried films were measured by surface profilometry (Alpha-Step 200, Tencor Instrument).

The structures of the final mesostructured films were characterized with TEM images and XRD patterns. TEM images of both 1.0 and 2.0 wt % SDS sol–gel films were taken. Calcination of the films at 400 °C for 4 h removes the surfactant. XRD patterns taken before and after calcination often assist in the determination of the kinds of mesostructures present in the films. Color changes are often observed in the calcined films, indicating the shrinkage of the films through the removal of surfactant.

**Probe Molecules.** The fluorescent molecular probe molecules used in this work are pyranine (trisodium 8-hydroxy-1,3,6-pyrenetrisulfonate)



and pyrene.



The protonated form of pyranine has an emission maximum at 430 nm (e.g. in alcohol) and the deprotonated form has a maximum at 510 nm (e.g. in water).<sup>11,12</sup> It has been used to monitor the alcohol/water ratios in sol–gel films.<sup>8</sup> The vibronic band intensity ratios of pyrene have been used previously to distinguish surfactant concentrations below and above the critical micelle concentration (cmc) in aqueous solu-

(6) Brinker, C. J.; Frye, G. C.; Hurd, A. J.; Ashley, C. S. *Thin Solid Films* **1991**, 201, 97.

(7) Brinker, C. J.; Hurd, A. J.; Schunk, P. R.; Frye, G. C.; Ashley, C. S. *J. Non-Cryst. Solids* **1992**, 147 & 148, 424.

(8) Nishida, F.; McKiernan, J. M.; Dunn, B.; Zink, J. I.; Brinker, C. J.; Hurd, A. J. *J. Am. Cer. Soc.* **1995**, 78, 1640.

(9) Brinker, C. J. et al. In *Access in Nanoporous Materials*; Pinnavaia, T. J., Thorpe, M. F., Eds.; Plenum: New York, 1995; p 123.

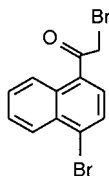
(10) Brinker, C. J.; Scherer, G. W. *Sol–Gel Science*; Academic: San Diego, 1990; p 120.

(11) Kaufman, V. R.; Avnir, D.; Pines-Rojanski, D.; Huppert, D. *J. Non-Cryst. Solids* **1988**, 99, 379.

(12) Clement, N. R.; Gould, M. *Biochemistry* **1981**, 20, 1534.

tions.<sup>13</sup> The incorporation of pyrene in spin-coated surfactant-templated sol–gel silica films has also been reported,<sup>14</sup> and its use as a probe of the pore environment in sol–gel materials has been reviewed.<sup>15</sup> Both probes are strongly luminescent.

Local molecular motions in the fresh dried SDS sol–gel films are probed by pyrene and a phosphorescent molecules BBAN (1-bromo-4-(bromoacetyl)naphthalene).



BBAN exhibits strong phosphorescence emission due to an efficient intersystem crossing mechanism of the bromonaphthyl ketone group.<sup>16</sup> The emission maximum for the broad BBAN phosphorescence band is centered around 440–442 nm. The phosphorescence lifetime of BBAN in glycerol at 20 °C is 2.23 ms.<sup>17</sup> The lifetime measured in a number of fluid solvents varied from a few milliseconds to hundreds of microseconds.<sup>17</sup> With BBAN's substantially longer emission lifetime, there is much more time for the probe to tumble before emission. Luminescence depolarization values of BBAN (i.e. phosphorescence depolarization) in the fresh dried film may be close to zero (i.e. scrambling of polarization of polarized excitation light due to probe molecules in all possible orientations at the time of emission).<sup>8</sup> The depolarization values will gradually increase as the probe becomes immobilized by the rigid structure of the film. Phosphorescence depolarization thus provides a measure of the local mobility of the molecular probe in the fresh dried films.

**Optical Measurements.** Emission spectra are combined with interferometry to study the dynamic physical and chemical changes that occur as the sol–gel films are deposited on the Si substrates. When the substrate is withdrawn from the solution at a constant rate, a steady state develops in a few seconds in which the film thickness at a given height above the solution remains constant even though the substrate is moving. The spectroscopic probing of the film formation process is carried out on the steady-state system. Illumination of the film with a monochromatic light causes constructive and destructive interferences of light rays reflecting off the top and bottom faces of the film, producing alternating bright bands and dark bands on the film.<sup>18</sup> Because the film thickness at a given height above the sol level is constant, the interference fringe pattern remains stationary even though the substrate is moving. Film thickness can thus be calculated from the fringe pattern.

The experimental arrangement was described previously.<sup>8</sup> A mercury lamp filtered to emit 546-nm light was placed at an angle of 35° to the substrate normal to illuminate the film. On the other side of the film, a telescope at an angle of 35° to the substrate normal was used to observe fringes in the film. Interference occurs at a thickness corresponding to

$$h = \frac{(2m + 1)\lambda}{4(n^2 - \sin^2\theta_L)^{1/2}} \quad (1)$$

where  $h$  is the film thickness,  $m$  is the interference fringe number,  $\theta_L$  is the illumination/viewing angle of the interference pattern, and  $n$  is the refractive index of the solvent and solid species at a location of

(13) Kalyanasundaram, K.; Thomas, J. K. *J. Am. Chem. Soc.* **1977**, *99*, 2039.

(14) (a) Ogawa, M. *Langmuir* **1995**, *11*, 4639. (b) Ogawa, M. *Chem. Mater.* **1998**, *10*, 1382.

(15) Dunn, B.; Zink, J. I. *Chem. Mater.* **1997**, *9*, 2280.

(16) (a) Bolt, J. D.; Turro, N. J. *Photochem. Photobiol.* **1982**, *5*, 305. (b) Turro, N. J.; Okubo, T.; Chung, C.-J. *J. Am. Chem. Soc.* **1982**, *104*, 1789.

(17) Marriott, G.; Jovin, T. M.; Yan-Marriott, Y. *Anal. Chem.* **1994**, *66*, 1490.

(18) Serway, R. A.; Faughn, J. S. *College Physics*; Saunders College Publishing: New York, 1992; p 817.

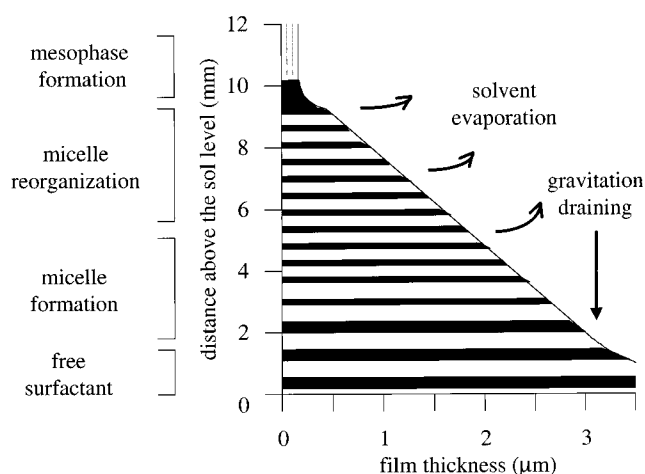


**Figure 1.** Schematic diagram of the film thickness profile of a SDS-templated sol–gel film and the interference fringe pattern that is generated when a monochromatic light illuminates the continuously thinning film. Also shown are the concurrent various stages of surfactant organization.

interest on the film.<sup>19</sup> On the basis of the measured thickness of the final film,  $m = 1$  for the last observable fringe.

The interference fringes were reproducible with identical pulling conditions. The last observable fringe is called the 0th fringe, or the drying line as used in earlier reports, beyond which the film microstructure is essentially established. The lower fringes are called the first fringe, second fringe, and so on. Continuous solvent evaporation shrinks the film. Each fringe above the sol represents a decrease in the thickness of about 2200 Å; this value varies with height above the sol because the refractive index increases during processing. The film thickness decreases to 1500 Å from an initial value of about 40 000 Å (or 4 μm) near the sol level. In addition to providing a measure of the film thickness, the fringes also serve as a convenient vertical and time scale. Both the time taken and height above the sol level to reach a point on the fringe pattern can be determined.

For all luminescence spectroscopic experiments the excitation source is the 351-nm polarized light from a Coherent Innova 90 Ar<sup>+</sup> laser (50:1 vertical polarization). The laser is focused to about 100 μm permitting excellent spatial resolution. The spot size is much smaller than the width of the fringe; changes in adjacent fringes can be easily located. The emission spectra were recorded by using an EG&G model 1420 optical multichannel analyzer and a 0.32 m Jobin-Yvon/ISA monochromator for dispersion. The slit width was 150 μm (or 20–50 μm for the pyranine experiments in the sol without surfactant due to the strong signal), and the integration time was 1 s. For the BBAN dried-film dynamics study, emission spectra were taken to measure the degree of phosphorescence depolarization over time. The polarized emission spectra were taken soon after film formation and continued for several hours to a day.

## Results and Discussion

One of the advantages of the film deposition process is the spatial and temporal separation of the chemical and structural processes leading to the formation of mesostructured sol–gel films. Figure 1 shows the schematic diagram of the film thickness profile of a SDS-templated sol–gel film and the interference fringe pattern that is generated when the film is illuminated by monochromatic light. Also shown are the various concurrent surfactant organization stages illustrating their spatial and temporal separation. The fringe pattern is stationary and the film thickness at a particular height above the sol level is constant, even though the substrate is constantly moving upward from the sol reservoir. A photograph of a characteristic fringe

(19) Ditchburn, R. W. *Light*, 3rd ed.; Academic Press: London, 1976; p 113.



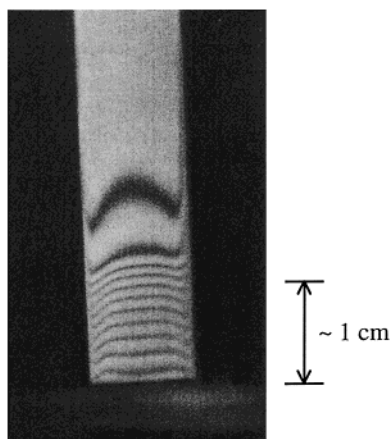


**Figure 2.** Photograph of an interference fringe pattern observed on a sol-gel thin film. The substrate is being withdrawn from a sol reservoir and is moving but the fringe pattern is constant.

pattern for the nonsurfactant sol-gel film as it is withdrawn from the reservoir is shown in Figure 2.

Probing these dynamic changes is achieved by adding a very low concentration of a suitable luminescent molecular probe to the sol, and taking the emission spectra or polarized emission intensities of the probe at various fringes on the developing film. The combination of interferometry and emission spectroscopy is used to probe the chemical and physical conditions at a particular point during the film development process.

Incorporation of luminescent molecular probes in the films not only allows in situ probing of the film formation process, but also results in luminescent mesostructured thin films. The probe molecules can be regarded as giving luminescence properties to these films. The films are stable at room temperature; they possess the same surface appearance and show the same XRD patterns after months of storage at room temperature.

**A. Film Structure.** Mesostructured silica films templated by SDS can be made by adding 0.5–2 wt % SDS to the TEOS sol. The films made with  $\leq 1.0$  wt % SDS are uniform in color (blue) and are 1500 Å thick, as measured by profilometry. Films made from sols with SDS concentrations  $\geq 1.5$  wt % contain some radial spots and stripes.

The structure in the films is characterized from TEM images. TEM images of 1.0 and 2.0 wt % SDS sol-gel films show regularly spaced layered structure with separation between adjacent layers ( $\sim 40$ – $45$  Å for 2 wt % SDS films) roughly corresponding to that found by the XRD patterns ( $\sim 42$  Å for 2 wt % SDS films).<sup>4</sup> Figures 3a and 3b show the lamellar phase structure of the SDS-templated sol-gel films and the TEM image of a 2.0 wt % SDS sol-gel film, respectively.

Calcination of the films at 400 °C for 4 h removes all the organic species. This procedure destroys the structure and leaves behind only the inorganic silica matrix. XRD patterns of the calcined films show loss of all the peaks. Mesostructured SDS sol-gel powders have also been reported to display lamellar structure with a  $d$ -spacing of 35 Å.<sup>20</sup>

Mesostructured sol-gel silica materials have been proposed to form by cooperative co-assembly of the inorganic silicate species and the organic surfactant aggregate during the course of the reaction.<sup>21–23</sup> In the case of an anionic surfactant  $S^-$  and the anionic inorganic silica  $I^-$ , the formation process is mediated

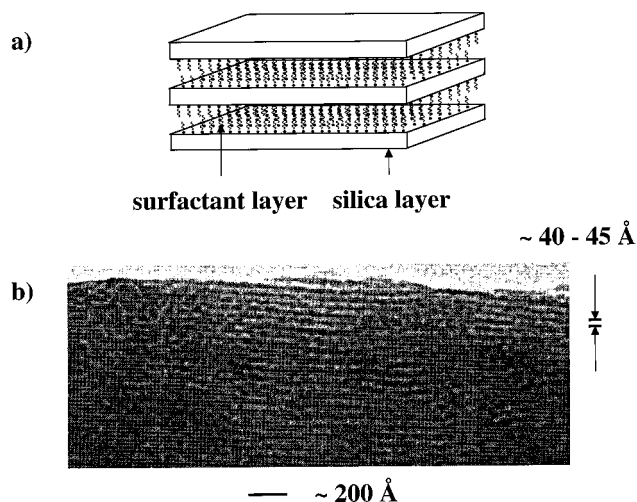


**Figure 3.** (a) Lamellar phase structure of the SDS-templated sol-gel film, consisting of alternating layers of silica layers and surfactant layers. The hydrophobic hydrocarbon tails face away from the silica layers. (b) TEM image of a 2.0 wt % SDS-templated sol-gel film, showing the ordered lamellar structure. The indicated distance represents the distance of each repeating organic and inorganic layer. It is estimated, from other TEM images, that the inorganic layer is about 5–10 Å thick.

by the cation  $Na^+$ , i.e.,  $S^-Na^+I^-$ . The proposed mechanism involves cooperative nucleation of the inorganic silicate and its interaction with the organic SDS surfactant by electrostatic forces followed by liquid crystal formation of the lamellar phase structure by SDS. The molecular inorganic silicate is arranged in a layered fashion imposed by the SDS lamellar structure. Finally, silicate polymerization and condensation form the final mesostructure. In the rapid film formation process, these stages probably overlap in time.

**B. Monitoring Changes in the Water Content.** The dynamic changes in the solvent composition that occur during film formation are monitored by in situ fluorescence spectra of the pyranine probe at various points on the developing film. The variation in the alcohol:water ratio during the film development is monitored by blue (430 nm) to green (510 nm) luminescence band intensity ratios of pyranine.<sup>8</sup> Variations in the water content for 1 wt % SDS sol-gel films and nonsurfactant sol-gel films (sol prepared the same way, but without addition of surfactant) have also been studied. Comparison of the results allows the effect of surfactant on the water content to be detected. A ternary composition diagram of the relative amount of water, alcohol, and silica can be mapped for both systems to show the different paths taken to make the final silica films.

The results of the variation in the water content for the nonsurfactant sol-gel films are summarized in Figure 4. The corresponding results for 1 wt % SDS sol-gel films are summarized to the left of the fringe pattern in Figure 5. Representative pyranine spectra obtained for some 1 wt % SDS sol-gel films are shown in Figure 6a.

In both of the above films, the water-to-alcohol ratio increases continuously during film development because of the higher vapor pressure and faster evaporation of alcohol.<sup>8</sup> In the nonsurfactant sol, the water content is about 2% and remains low until the final stage of the processing (second fringe, 10–

(20) Yada, M.; Kitamura, H.; Machida, M.; Kijima, T. *Langmuir* **1997**, 13, 5252.

(21) Huo, Q.; Margolese, D. I.; Ciesla, U.; Demuth, D. G.; Feng, P.; Gier, T. E.; Sieger, P.; Firouzi, A.; Chmelka, B. F.; Schüth, F.; Stucky, G. D. *Chem. Mater.* **1994**, 6, 1176.

(22) Huo, Q.; Margolese, D. I.; Ciesla, U.; Feng, P.; Gier, T. E.; Sieger, P.; Leon, M. R.; Petroff, P. M.; Schüth, F.; Stucky, G. D. *Nature* **1994**, 368, 317.

(23) Raman, N. K.; Anderson, M. T.; Brinker, C. J. *Chem. Mater.* **1996**, 8, 1682.

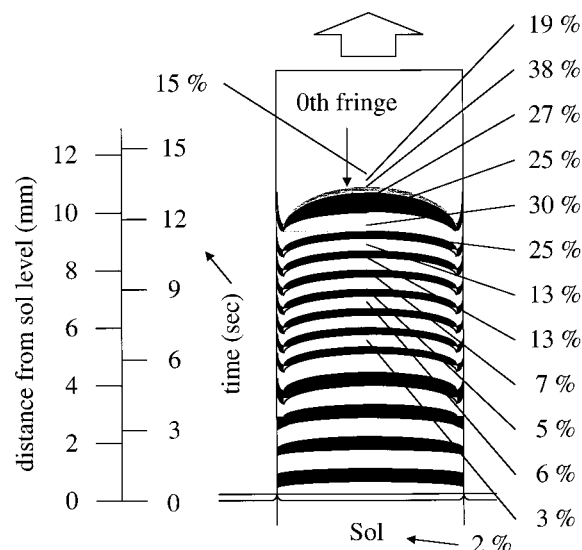


**Figure 4.** Schematic diagram of the results of the interferometry and spectroscopy of nonsurfactant sol-gel films. The steady-state fringes are shown by dark bands. The distance from the sol in millimeters and the processing time in seconds are shown at the left. The values of percent water as a function of film thickness are shown to the right of the film.

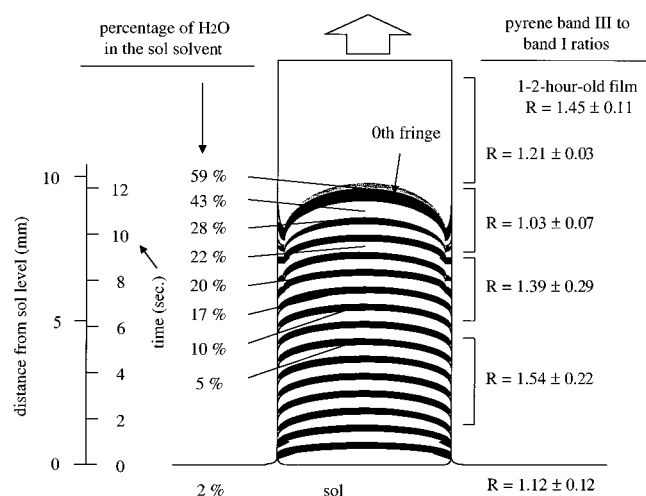


**Figure 5.** Schematic diagram of the results of the interferometry and spectroscopy of 1 wt % SDS sol-gel films. The distance from the sol in millimeters and the processing time in seconds are shown at the left. The percent water as a function of film thickness and processing time are shown to the left of the film. The pyrene vibronic band intensity ratios  $R$  that are used to determine polarity are shown on the right.

11 s), where it reaches about 13%. The water content then increases to about 25–30% in the final stage of the film formation process (the region from the first fringe to the fringe, 11–13 s). Near the top of the fringe, the water content is close to 40%.

Substantially higher water content in the depositing film is measured when SDS is added to the sol. In the 1 wt % SDS sol, the water content is about 2%, but about halfway through the processing (sixth fringe, 6 s) it has increased to about 10%. By the time the film has shrunk to nearly its final thickness (fringe, 12 s) it has increased to almost 60%. The finding of high water content near the end of the SDS film formation process is similar to those obtained from the nonsurfactant film, indicating that the presence of surfactant in the sol does not alter the trend in the evolution of the solvent composition during film development.

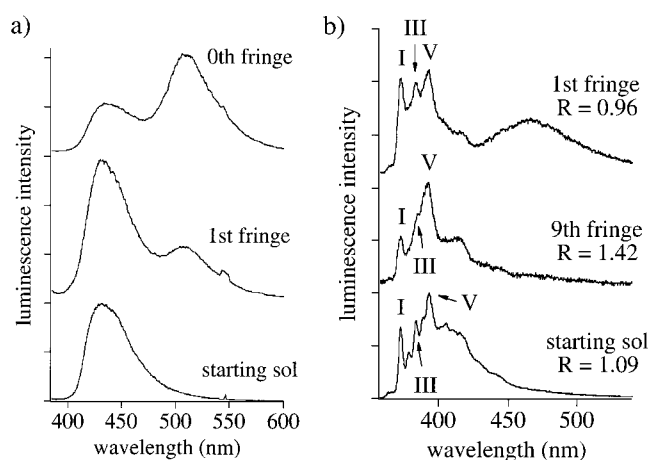


**Figure 6.** (a) Representative spectra of the pyranine probe that are used to calculate the percent water at three different positions. (b) Representative pyrene spectra from which  $R$  values are obtained are shown. Note the increase, decrease, and final increase in  $R$  as a function of time, indicative of micelle formation followed by breakup and re-formation.

The substantially higher water content measured in the 1 wt % SDS films (i.e. ~60% in the SDS films vs 25–30% in the nonsurfactant films) can be explained in terms of the anionic probe molecules experiencing a greater amount of water near the sodium cations in the vicinity of the polar end of the anionic surfactant molecules. By the time the final lamellar structure is formed (see next section), there is an organized micellar structure present in the film. Sodium ions are probably close to the polar end of the anionic surfactant to act as the mediating species and facilitate the formation of the final ordered structure in the film.<sup>21</sup> There is probably a greater local concentration of water in this region as detected by the pyranine molecules than on the film lacking the surfactant. Solvation of the ions<sup>24</sup> may also help to retain water more effectively than alcohol, resulting in the higher water content that is measured at the final stage of the SDS film formation process.

On the basis of the difference in the evolution of solvent composition for the surfactant and nonsurfactant systems, different paths are followed by the two systems during film formation. A ternary composition diagram with the percentages of silica, water, and ethanol is used to illustrate the paths in Figure 7. In both systems not much change has occurred until around halfway through the processing (see the next section for silica evolution), so the sol composition remains at the starting point of the curved line. The nonsurfactant sol follows a straighter path to form the final silica films, due to the relatively small change in the solvent composition throughout most of the film formation process. The SDS sol follows a more curved path, tending toward the higher water content region of the triangle. After the sol has reached the final formation stage with its maximum water content, the processing path moves straight toward the silica side to form the final surfactant-templated silica films.

It is interesting to compare the above results of water content to those obtained for a pure TEOS sol.<sup>8</sup> The greater the amount of water that is present in the starting sol, the greater the percentage of water near the fringe. The solvent near the fringe is almost all water in films pulled from the starting pure TEOS sol containing 12.5 vol % water. Water content only rises to

(24) Radel, S. R.; Navidi, M. H. *Chemistry*; West Publishing Company: New York, 1990; p 533.

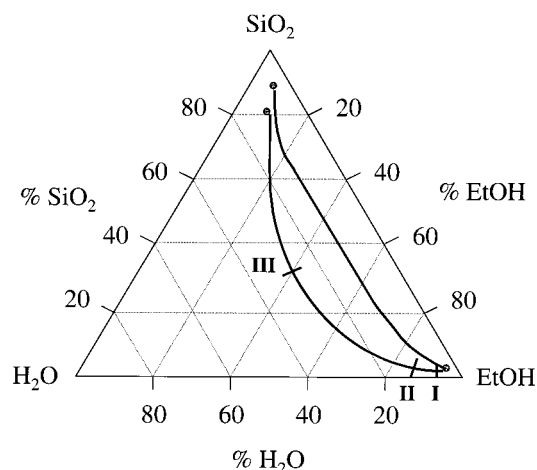


**Figure 7.** Ternary composition diagram of the percentages of silica, water, and ethanol. Film formation paths taken by the two sols are shown. The straighter line (right side) is the path for the nonsurfactant sol-gel films. The curved line (left side) is the path taken by the SDS sol-gel films. Stages of the surfactant organization are labeled along the path for the SDS sol-gel films: (I) micelle formation, (II) micelle disruption and reorganization starts, and (III) lamellar mesophase formation.

about 60% at the fringe from the starting SDS sol containing just 5.7 vol % water.

**C. Monitoring Micelle and Mesophase Formation.** Micelle formation is probed during film formation by the vibronic band intensity ratios in the emission spectrum of pyrene. The results of the variation in the intensity ratio  $R$  are shown on the right side of the fringe pattern in Figure 5. The experimental uncertainty in the III/I ratio recorded in each bracketed region represents the range of the ratios measured. The  $R$  value given is the average ratio in that particular region. The results of the probe of micelle formation are surprising: micelle formation occurs almost immediately above the sol, but the micelle is broken up about halfway through the film formation and only forms the final lamellar structure at the very end of the processing. Representative pyrene spectra are shown in Figure 6b.

In considering the micelle and final lamellar phase formation, it is important to take into account the effect of the forces acting on the depositing film that give it the shrinking film profile. These forces include gravitational draining, solvent evaporation, and shrinkage. The presence of silicate oligomers in the film that grow along with micellar structure should be considered as well.

The III/I ratio of pyrene in the starting sol is  $1.12 \pm 0.12$ . The same value is measured when the surfactant is absent. The value in pure ethanol is 0.91 and that in pure water is 0.63.<sup>13</sup> Thus, micelles are not present in the starting sol and pyrene is responding to a polar environment. Between about 2 and 5 s during the film formation, the ratio dramatically increases to  $1.54 \pm 0.22$ . This increased value is indicative of a nonpolar environment and signals micelle formation. (The ratio is 1.65 in hexane.<sup>13</sup>) In the first two seconds of the film-forming process, gravitational draining probably dominates solvent evaporation. All species, including surfactant, solvent, and silicate oligomers, are continuously draining back down to the sol reservoir. Surfactant concentration does not exceed cmc and the flow of materials in the film inhibits the formation of micelles. However, at later times higher in the developing film, solvent evaporation becomes progressively dominant in its effect on film shrinkage. At this point the solid species (surfactant

molecules and silicate oligomers) are starting to be retained in the film. Solvent composition outside of the micelle has not changed dramatically, but the film thickness has shrunk from about 3  $\mu\text{m}$  to 2  $\mu\text{m}$  (from the initial film just above the sol reservoir to the 12th fringe), the surfactant concentration has increased, and the critical micelle concentration (cmc) is exceeded.

As the film development proceeds, the ratio surprisingly decreases back to a value about that of the original sol. This transition to a low ratio value begins about 6 s into the film development at about the sixth fringe. In this region the film thickness continues to decrease and the percent water concentration markedly increases. Silicate concentration also increases due to film shrinkage. A likely explanation of the decrease in the ratio is that the originally formed micelle is disrupted and the structure is undergoing a phase change, typical of surfactant behavior in aqueous solution as the surfactant concentration increases.<sup>25</sup> As these changes occur, the pyrene is reexposed to the solvent and the ratio reports the significant increase in polarity. The high water concentration near the final stage of film formation may account for the extremely low III/I ratio measured (1.03). Water decreases the III/I ratio more than alcohol does.

During the transitional period in the presence of silicate species, it is possible that SDS may not exhibit distinct hexagonal or cubic phases but rather may form the lamellar structure from some semiorganized structure.<sup>26</sup> Certain surfactants (such as some short-chain surfactants)<sup>21</sup> that form hexagonal phase structures do so to form elongated micellar rods in the intermediate stage. Some kind of micellar structure may be present in the SDS film, and it may evolve continuously in response to the growing concentration of surfactant as the film shrinks. Pyrene can be exposed to the solvent during this process.

Finally, at and above the fringe, the pyrene again becomes contained in a nonpolar environment as the final lamellar phase is formed. However, the largest values do not occur immediately at the final fringe (where the film almost reaches its final thickness) but rather require an additional 5–15 min. There are still dynamic processes occurring during this time such as continued solvent evaporation and/or flexibility of the surfactant in the lamellar structure, contributing to the slow increase in the ratio. The ratio measured after 1–2 h is  $1.45 \pm 0.11$ . The final ratio of the fully developed film measured after several weeks is 1.67.

A likely possibility for the final lamellar phase formation is the spontaneous organization into the lamellar structure with silica when the surfactant concentration of the micellar structure in the transformation period has exceeded a sufficient concentration. The various stages of micelle formation, transformation, and final formation of the lamellar structure during film formation are shown on the ternary composition diagram in Figure 7.

**D. Local Mobility in the Final Film.** The spectra of the pyrene probe provide additional insight concerning the molecular motion above the fringe; a broad excimer peak caused by dimerization in the excited state grows at about the zeroth fringe and then decreases during a period of several hours. The excimer

(25) (a) Ross, S.; Morrison, I. D. *Colloid Systems and Interfaces*; John Wiley & Sons: New York 1988; p 173. (b) Myers, D. *Surfactant Science and Technology*; VCH Publishers: New York 1988; p 81. (c) Clint, J. H. *Surfactant Aggregation*; Chapman and Hall, Inc.: New York, 1992; p 147. (d) Rosen, M. J. *Surfactants and Interfacial Phenomena*, 2nd ed.; John Wiley & Sons: New York, 1989; p 108.

(26) Kaufman, V. R.; Avnir, D. *Langmuir* **1986**, 2, 717.



peak is centered around 465 nm. The excimer peak first appears when the laser excites the molecules in the region of the first fringe, as shown in Figure 6b, grows in intensity further up the film, and then slowly decreases. (The maximum excimer peak intensity grows to about the height of peak V in the monomer fluorescence around 6 s after film formation. Then the peak intensity decreases to half its maximum intensity in about 60 min and continues to decrease for several hours.) These results suggest that at the first fringe the pyrene concentration becomes high enough to allow excimer formation to occur because of the large reduction in the film volume. As the lamellar structure forms, the pyrene molecules become immobilized and isolated; the continuous decrease in mobility with time inhibits the excimer formation.<sup>26</sup>

XRD patterns, taken at 8-min intervals over 2 h, were used to investigate whether long-time structural changes occurred. No measurable changes were observed. These results suggest that the long-range order of the lamellar structure is established at about the time the final thickness is reached even though more local dynamics persist for several hours.

To further study the local molecular dynamics within the hydrocarbon chains of the surfactant layers in the final films, another probe, BBAN, was employed. Phosphorescence depolarization experiments show that BBAN is essentially immobile at the fringe. These results suggest that rotational motion of the planar probe molecule in the layered structure is largely inhibited, but translational motion along the hydrocarbon planes may be possible, as evidenced by the mobility of the pyrene excimer in the film.

### Summary

SDS-templated mesostructured sol–gel thin films formed by the rapid dip-coating method possess a highly ordered lamellar phase structure. XRD patterns and TEM images of the mesostructured sol–gel films confirm the existence of the ordered structures. The dynamic chemical and structural changes occurring during the pure and mesostructured sol–gel film formation are conveniently studied by the use of incorporated luminescent probes. By taking luminescence spectra of the probes at various points on the interference fringe pattern of a developing film, these changes can be followed.

Pyranine responds to the alcohol:water ratio in the sol. In both nonsurfactant silica films and SDS-templated sol–gel films preferential evaporation of alcohol gives a water-rich film near the end of the film development. Water content for 1 wt % SDS films increases progressively from about 2% in the sol to nearly 60% at the fringe. The water content is higher when SDS is added to the sol because of a greater amount of water near the sodium ions at the polar end of the anionic surfactant molecules.

Pyrene's sensitivity to the polarity of its immediate environment is employed to monitor micelle formation. The results provide evidence of micelle formation, breakup, and its transformation to the final lamellar structured films. The changes in pyrene excimer peak intensity indicate molecular mobility in the fresh-dried SDS films. Pyrene excimer emission provides a measure of the local molecular mobility in the fresh-dried films. Local mobility, probably caused by the flexibility in the hydrophobic tails of the surfactant, persists for hours after film formation.

Finally, it should be noted that incorporation of luminescent dyes in the films not only allows detection of the processes involved to form these mesostructured sol–gel films, but the films themselves can also be regarded as possessing luminescence properties. When combining the knowledge gained through the *in situ* luminescence studies with the characterizations of the final dried films by XRD patterns, TEM images, and other techniques, a more complete understanding of the processes occurring during the dip-coating process is possible. This understanding can lead to a better design of mesostructured sol–gel films in the future with the desired structures and properties, and lead to the realization of possible applications.

**Acknowledgment.** The authors thank Dr. C. Jeffrey Brinker at the Sandia National Laboratories and the University of New Mexico for the helpful suggestions about the ternary composition diagram and for taking the TEM images of the SDS films. This work was supported by a grant from the National Science Foundation (DMR9729186) with additional support from Sandia National Laboratories (AV-1153).

JA993882E